

MOL #72322

Miltefosine Induces Apoptosis-like Cell Death in Yeast via Cox9p in Cytochrome c Oxidase

**Xiaoming Zuo, Julianne T. Djordjevic, Johanes Bijosono Oei, Desmarini Desmarini,
Stephen D. Schibeci, Katrina A. Jolliffe, and Tania C. Sorrell**

*Centre for Infectious Diseases and Microbiology, Westmead Millennium Institute and Sydney
Emerging Infections and Biosecurity Institute, University of Sydney, NSW 2145, Australia (X.Z.,
J.T.D., J.B.O., D.D., T.C.S.); Institute for Immunology and Allergy Research, Westmead
Millennium Institute, University of Sydney, NSW 2145, Australia (S.D.S.) and School of
Chemistry, University of Sydney, NSW 2006, Australia (K.A.J.)*

MOL #72322

Running title: Miltefosine Induces Apoptosis-Like Cell Death in Yeast

Corresponding author: Tania C. Sorrell. Centre for Infectious Diseases and Microbiology,
Westmead Millennium Institute and Sydney Emerging Infections and Biosecurity Institute,
University of Sydney, NSW 2145, Australia. Phone: (+61) 2 9845 6012. Fax: (+61) 2 9891 5317.
E-mail: tania.sorrell@sydney.edu.au

Number of text pages: 40

Number of tables: 3

Number of figures: 6

Number of references: 40

Number of words: Abstract, 146; Introduction, 639; Discussion, 1409

Abbreviations: COX, cytochrome c oxidase; PC, phosphatidylcholine; MIC, minimum inhibitory concentrations; MFC, minimum fungicidal concentration; PE, phosphatidylethanolamine; TUNEL, terminal deoxynucleotidyl transferase dUTP nick end labeling; AEBSEF, 4-[2-aminoethyl]-benzene-sulfonylfluoride.HCl; PI, propidium iodide; WT, wild type; SSC, side scatter

MOL #72322

Abstract

Miltefosine has antifungal properties and potential for development as a therapeutic for invasive fungal infections. However, its mode of action in fungi is poorly understood. We demonstrate that miltefosine is rapidly incorporated into yeast where it penetrates the mitochondrial inner membrane, disrupting mitochondrial membrane potential and leading to an apoptosis-like cell death. *COX9*, which encodes subunit VIIa of the cytochrome c oxidase (COX) complex in the electron transport chain of the mitochondrial membrane, was identified as a potential target of miltefosine from a genomic library screen of the model yeast *Saccharomyces cerevisiae*. When over-expressed in *S. cerevisiae*, *COX9*, but not *COX7* or *COX8*, led to a miltefosine-resistant phenotype. The effect of miltefosine on COX activity was assessed in cells expressing different levels of *COX9*. Miltefosine inhibited COX activity in a dose-dependent manner in Cox9p-positive cells. This inhibition most likely contributed to the miltefosine-induced apoptosis-like cell death.

MOL #72322

Introduction

Invasive fungal infections are associated with high morbidity and mortality and are an increasing global health problem. Current therapies are limited in efficacy, antifungal spectrum and/or safety and resistant fungi are emerging. Hence there is an urgent need for new agents. Several novel potential antifungal targets have been identified in recent years yet only one new class of drug, the echinocandins, has been marketed (Chen and Sorrell, 2007).

Recently, our group demonstrated that miltefosine (2-[hexadecoxy-oxido-phosphinoyl]oxyethyl-trimethyl-ammonium), which is an alkyl phospholipid and metabolically stable analogue of the major eukaryotic cell membrane phospholipid, phosphatidylcholine (PC) (van Blitterswijk and Verheij, 2008), has broad spectrum antifungal activity. Miltefosine was first investigated as an anticancer agent (Unger and Eibl, 1991) and later developed and marketed as an oral treatment for the parasitic disease, leishmaniasis (Croft et al., 2003; de Castro et al., 2004).

Against fungi, minimum inhibitory and fungicidal concentrations (MICs / MFCs) of miltefosine were comparable to those of the commonly used drug, amphotericin B (Widmer et al., 2006b). Miltefosine was also broadly active against dermatophytes (Tong et al., 2007). The MICs against most pathogenic fungi were well below serum levels achieved by oral miltefosine dosing (Obando et al., 2007). In a single case report, the addition of miltefosine to other antifungal agents as salvage therapy proved effective for treatment of *Scedosporium prolificans* osteomyelitis (Kesson et al., 2009). Although miltefosine shows promise as an antifungal drug, its mode of action is yet to be elucidated, but is the key to rational design of more potent and less toxic analogues.

MOL #72322

Most of what is known about the mechanism of action of miltefosine comes from studies performed in neoplastic cells (van Blitterswijk and Verheij, 2008) and *Leishmania* (Barratt et al., 2009). These have revealed a number of poorly defined mechanisms, different between mammalian and parasitic cells. In neoplastic cell lines, miltefosine is internalized mainly via receptor-independent, membrane-recycling endocytosis, whereas in *Leishmania* it is primarily via a specific membrane transporter, LdMT-LdRos3, a two subunit aminophospholipid translocase with P-type ATPase activity (Perez-Victoria et al., 2003).

In neoplastic cell lines, because of its phospholipid-like structure, miltefosine is believed to exert its antiproliferative effect by interfering with lipid rafts and proteins in cell membranes. Miltefosine has been reported to inhibit enzymes involved in phospholipid metabolism, including protein kinase C; phospholipases A₂, C and D; and choline-phosphate cytidylyltransferase in the PC biosynthesis pathway. Miltefosine also triggers signaling pathways that lead to apoptosis (Ruiter et al., 1999) and, at high concentrations, forms pore-like structures on cell membranes, resulting in release of intracellular contents and impairment of cellular homeostasis (Wieder et al., 1999). In *Leishmania*, miltefosine inhibits both phosphatidylethanolamine (PE) *N*-methyltransferase in the PC synthetic pathway and a glycosome-located alkyl-specific acyl coenzyme A acyltransferase involved in lipid remodeling (Lux et al., 2000; Urbina, 2006) and has been reported to induce apoptosis (Verma et al., 2007).

In the model yeast, *Saccharomyces cerevisiae*, deletion of the drug-specific transporter Lem3p, a functional homologue of the leishmanial LdMT-LdRos3, conferred resistance to miltefosine and reduced uptake of fluorescently labeled derivatives of PC and PE, suggesting that alkyl phospholipid analogues including miltefosine are internalized via Lem3p (Hanson et al., 2003). We showed previously that miltefosine inhibits phospholipase B1, a key virulence

MOL #72322

determinant of the pathogenic yeast-like fungus, *Cryptococcus neoformans*, but only at relatively high concentrations, suggesting that this is not its primary mode of action (Widmer et al., 2006b). The fungal cell targets of miltefosine are still unknown.

In this study, we demonstrate in *S. cerevisiae* that miltefosine is taken up rapidly and penetrates the mitochondrial inner membrane, where it disrupts membrane potential and causes dose-dependent inhibition of cytochrome c oxidase (COX) and apoptosis-like cell death. We also present evidence that the inhibition of COX by miltefosine occurs specifically at the site of subunit VIIa in the enzyme complex, which is encoded by a nuclear gene *COX9*.

MOL #72322

Materials and Methods

Strains, Media and Manipulations

Yeast strains used in the work are listed in Table 1. For yeast culture, complete medium contained 1% Bacto yeast extract (Becton Dickinson, USA) and 2% Bacto peptone (Becton Dickinson, USA) with 2% glucose (YPD) or glycerol (YPGly). For determination of growth on solid media, 2% Bacto agar was added. Minimal medium (YNB) contained 2% glucose and 0.67% Difco yeast nitrogen base (Becton Dickinson, USA) without amino acids. Nutrients essential for propagation of auxotrophic strains were added to YNB at 25 µg/ml for uracil and adenine, and 50 µg/ml for leucine. For selection of geneticin resistance, the antibiotic was added to YPD at the concentration of 200 µg/ml. Standard methods were used for yeast incubation, transformation and DNA extraction (Burke et al., 2000).

Commercial MAX Efficiency DH5α Competent Cells (Invitrogen, Australia) were used as host for plasmid propagation in *Escherichia coli*. Luria Broth (LB, Sigma-Aldrich, Australia) was utilized for bacterial culture and ampicillin was added to the culture at a final concentration of 100 µg/ml to retain plasmids containing ampicillin resistance marker. A QIAprep Spin Miniprep Kit (Qiagen, Australia) was used to extract plasmid DNA from *E. coli*.

Standard methods were used for DNA restriction enzyme digestion, ligation and electrophoresis (Sambrook et al., 2001).

Measurement of Miltefosine Uptake

To measure miltefosine incorporation, strain M2915-6A was cultured at 30°C to a final cell density of 1×10^8 cells/ml (late log or early stationary phase) in a total of 50 ml of YNB broth

MOL #72322

supplemented with leucine, adenine and uracil. ^{14}C -labeled miltefosine (42 m Ci/mmol, GE Healthcare, USA) was mixed with non-labeled miltefosine (Cayman Chemical Co., USA) and the mixture was added to the yeast culture to give a final miltefosine concentration of 1 $\mu\text{g/ml}$ with a ^{14}C activity of 0.11 $\mu\text{Ci/ml}$. At 5 min intervals, 1 ml of culture was removed and the cells were pelleted by centrifugation. The supernatant, containing unincorporated ^{14}C -miltefosine, was collected and retained. The cells were immediately washed with 1 ml of phosphate buffered saline (PBS, Invitrogen, Australia) containing 10 mg/ml bovine serum albumin (BSA) to remove non-specifically bound drug from the surface, and the final cell pellet was dissolved in 500 μl of NCS tissue solubilizer (GE Healthcare, USA). The buffer used to wash the cells was combined with previously retained supernatant for measuring unincorporated ^{14}C -miltefosine. The solubilized cells and the combined supernatants were each mixed with 6 ml of Ultima Gold scintillant (PerkinElmer, USA) and analyzed in a Tri-Carb Liquid Scintillation Analyzer (Model 2100TR, Packard, USA) to obtain a measurement of cell incorporated and unincorporated ^{14}C -miltefosine respectively. Miltefosine uptake was expressed as the percentage of radioactivity incorporated by cells at each time point.

Assay of Cell Sensitivity to Miltefosine

Strain M2915-6A was cultured in YPD broth at 30°C to log phase. Cells were then harvested and resuspended in fresh YPD or YPGly at the density of 1×10^5 cells/ml. The cell suspensions were distributed into a 96-well plate at 50 $\mu\text{l/well}$. YPD or YPGly containing series concentrations of miltefosine was added and mixed with the cell suspensions to make the final volume 100 μl in each well and the drug concentrations from 0 to 256 $\mu\text{g/ml}$. The plate was then incubated in a moisturized container at 30°C for 4 days with vigorous shaking until the live cells

MOL #72322

reached the final stage of growth. Miltefosine sensitivity was assessed as the minimum drug concentration at which the cells were unable to grow.

Fluorescence Microscopy

Yeast cells were incubated in YPD broth with or without miltefosine at 2 $\mu\text{g/ml}$ for 1 h and then stained with DAPI (Invitrogen, Australia) to visualize mitochondrial nucleoids and nuclei. DiOC₆ (Invitrogen, Australia) and propidium iodide (PI, Invitrogen, Australia) were also added to detect mitochondrial membrane potential and permeability of the cell membrane, according to previous publications (Barcellona et al., 1990; Pringle et al., 1989). Briefly, yeast cells were harvested from the cultures, washed with water, and incubated for 20 min with DAPI, DiOC₆ and PI at concentrations of 2 $\mu\text{g/ml}$, 0.64 ng/ml and 10 $\mu\text{g/ml}$ respectively. To immobilize cells, an equal volume of 1% low melting temperature agarose (Roche, Australia), preheated at 35°C, was mixed with the stained cells prior to the application of the samples to the glass slides. Fluorescence was visualized under a DeltaVision RT Deconvolution Microscope System (Applied Precision, USA) fitted with a 100 \times oil/1.40 objective lens (Olympus, Japan). For DAPI, DiOC₆ and PI, the excitation/emission filters were set at 360/457, 490/528 and 555/617 nm respectively. Images were acquired using Resolve3D softWoRx (Applied Precision, USA, version 3.7.1) and Image J (<http://rsb.info.nih.gov/ij/>, version 1.43) at 1000 \times magnification, and assembled with Photoshop (Adobe, version 10.0) and Illustrator (Adobe, version 13.0).

Assessment of Apoptosis

Apoptosis was assessed using the Vybrant FAM Caspase Assay Kit (Invitrogen, Australia) and the *In Situ* Cell Death Detection Kit (TUNEL assay, Roche, Australia). Yeast cells were

MOL #72322

cultured in YPD broth to late log phase. Two aliquots of 2.4×10^8 cells were collected by centrifugation, washed with water and resuspended in 240 ml of YPD broth with and without 2 $\mu\text{g/ml}$ miltefosine. This concentration of miltefosine was inhibitory, but not lethal, to yeast cells since growth curves remained flat over a 4 h co-incubation period (data not shown). Apoptosis was measured in cultures that were incubated at 30°C with shaking. For the terminal deoxynucleotidyl transferase dUTP nick end labeling (TUNEL) assay, cells were fixed with 4% paraformaldehyde in PBS for 60 min and the cell walls were removed by digestion with 10 mg/ml Zymolyase-20T (MP Biomedicals, Australia) for 2 h at 37°C with mild shaking. The resulting spheroplasts were then treated with TUNEL reagents according to manufacturer's instructions. For the caspase assay, live cells were labeled directly with the caspase assay reagents and 10 $\mu\text{g/ml}$ PI according to the instruction manual. Flow cytometry was conducted by measuring 1.5×10^4 fluorescently labeled cells on a LSRII Flow Cytometer (BD Biosciences, USA). Labeled cells were also examined by fluorescence microscopy.

Genomic Library Construction and Screening

A genomic library from strain 6A-MI50-401 was constructed using a previously published method with modifications (Jauert et al., 2005). Genomic DNA was extracted and subjected to treatment with the restriction enzyme *EcoRI*. To preserve genes potentially containing *EcoRI* sites, the genomic DNA was partially digested. Fragments ranging in size from 100 bp to 10 kb were purified using a QIAquick PCR purification kit (Qiagen, Australia) and ligated into *EcoRI*-digested pCXJ15. The ligation mixture was used to transform MAX Efficiency DH5 α Competent Cells. Plasmid DNA was extracted from ampicillin resistant colonies which had grown on LB/ampicillin agar plates for 15 h at 37°C, and the DNA concentration was adjusted to 200

MOL #72322

µg/ml. The plasmid DNA from ten individual transformations was then pooled to form the final genomic library. The quality of the library was validated by comparing the electrophoresis profile of the *Eco*RI-released library inserts with that of the *Eco*RI-digested genomic DNA.

To screen for genes whose over-expression confers miltefosine resistance in yeast, strain M2915-6A was transformed with the resulting genomic library. Ura⁺ transformants were first grown on YNB agar plates without uracil at 30°C until the average colony size reached approximately 2 mm in diameter. The colonies were then replica plated onto YNB plates containing 20 µg/ml miltefosine and incubated at 30°C for 2 days. Ura⁺ colonies that also grew in the presence of miltefosine were selected and their resistance phenotype was confirmed by performing a serial dilution drop test (Zuo et al., 2007) on YNB containing miltefosine. Total DNA containing the plasmids from the miltefosine resistant isolates was purified and used to transform the MAX Efficiency DH5α Competent Cells. Plasmid DNA was then retrieved from the resulting ampicillin resistant colonies. The genomic inserts conferring the miltefosine resistance phenotype were then determined by DNA sequencing and BLAST search in the *Saccharomyces cerevisiae* Genome Database (<http://www.yeastgenome.org/>).

Cloning of *COX7* and *COX8*

PCR fragments containing *COX7* or *COX8* were amplified using primer pairs ScCOX7 FP1 and ScCOX7 RP1 or ScCOX8 FP1 and ScCOX8 RP1 (Table 2), respectively. An *Eco*RI site was designed at the 5' end of each primer. PCR reactions were conducted using a T-Gradient PCR machine (Biometra, Germany) with standard protocol. Products of *COX7* and *COX8* genes both with a size of 1.2 kb were treated with *Eco*RI and ligated into the corresponding site of pCXJ15 to generate pCXJ15-COX7 and pCXJ15-COX8 respectively.

MOL #72322

Quantitative Real Time PCR

Total RNA was prepared from yeast transformants 6A-[pCXJ15-COX7], 6A-[pCXJ15-COX8], 6A-[pCXJ15-COX9] and 6A-[pCXJ15] using TRIzol reagent (Invitrogen, Australia) following the manufacturer's instructions. RNA concentration and purity were determined using a NanoPhotometer (Implen, Germany) and an A_{260}/A_{280} ratio of 1.9 or greater was indicative of a sufficient purity for qRT-PCR. An amount of 5 μ g of total RNA from each strain was treated with DNase I (Amplification Grade, Invitrogen, Australia) and used as a template for oligo-dT-primed cDNA synthesis using the SuperScript III First-Strand Synthesis System (Invitrogen, Australia). RNase H (Invitrogen, Australia) was then used to remove the RNA component in the RNA/cDNA complex. Standard curves were prepared using equal amounts of cDNA from all strains to obtain final concentrations of 100, 20, 4, 0.8 and 0.16 ng/ μ l. For individual samples, cDNA from each strain was diluted to a final concentration of 4 ng/ μ l. A volume of 5 μ l of each standard and sample was then used as a template for qRT-PCR using Platinum SYBR Green qPCR SuperMix-UDG (Invitrogen, Australia). The primers used are listed in Table 2. The PCR conditions were adjusted in accordance with the instructions from the manufacturers. Thermo cycling was set at 95 °C for 15 sec and 60 °C for 45 sec, and a total of 40 cycles were conducted on a Rotor-Gene 6000 RT-PCR machine (Corbett Research, Australia). Data were then obtained and analyzed using the Rotor-Gene 6000 Series software (version 1.7, Corbett Research, Australia). For all tested transformants, *COX* gene expressions were normalized to the expression of a house-keeping gene, *ACT1*, using the standard curves and calculated by taking the expressions in 6A-[pCXJ15] as basal levels.

MOL #72322

COX9 Deletion

To generate a Δcox9 null mutant in the background of M2915-6A, a PCR based method using a *KanMX4* cassette (Wach et al., 1994) was used to disrupt *COX9* in the strain. A 2.1 kb fragment containing *KanMX4* disrupted *COX9* ($\text{cox9}\Delta::\text{KanMX4}$) was amplified from the commercially available strain, BY4741/ Δcox9 (Open Biosystems, USA). The primers used were Sc *cox9* FP1 and Sc *cox9* RP1 (Table 2). The PCR product was then transformed into M2915-6A to replace the endogenous 0.7 kb *COX9* region by homologous recombination. Δcox9 mutants were selected on the basis of stable geneticin resistance. To confirm disruption of *COX9*, PCR primer pair Sc *cox9* FP2 and Sc *cox9* RP2 (Table 2), annealing to the 5' and 3' flanking sequences of the disrupted locus respectively, was used to visualize a 2.5 kb DNA fragment in place of a 1.1 kb in the WT.

Preparation of Mitochondria and Post-Mitochondrial Membranes

Mitochondrial fractions were prepared from 500 ml cultures grown to late log phase in YPD broth at 30°C (Clark-Walker et al., 2000). Briefly, cells were harvested, resuspended in 30 ml of suspension buffer (1.2 M sorbitol, 20 mM *N*-Tris [hydroxymethyl] methyl-2-aminoethanesulphonic acid [TES], 14 mM β -mercaptoethanol, pH 7.4) containing 10 mg/ml Zymolyase-20T and incubated at 35°C for 60 min to allow cell wall digestion. The resulting spheroplasts were resuspended in 30 ml of ice cold homogenization buffer (0.6 M sorbitol, 10 mM TES, 0.1 mM 4-[2-aminoethyl]-benzene-sulfonylfluoride.HCl [AEBSF], pH 7.4) and ruptured in a Dounce homogenizer with 30 strokes. Mitochondria were pelleted by centrifugation at $9000 \times g$ for 20 min after prior removal of cellular debris by two 5-min rounds of centrifugation at 3500 and $5000 \times g$ respectively. Mitochondria were resuspended in 200 μ l of

MOL #72322

mitochondrion buffer (5 mM TES, 150 mg/ml glycerol, 0.5 mM EDTA, 0.5 mM dithiothreitol, 0.1 mM AEBSF, pH7.5) and stored at -80°C . The post-mitochondrial supernatant was then centrifuged at $100,000 \times g$ to obtain membrane enriched pellet.

COX Assay

A commercial Cytochrome c Oxidase Assay Kit (Sigma-Aldrich, Australia) was used to measure the enzyme activity in mitochondrial fractions and examine the inhibition of the enzyme by KCN (Sigma-Aldrich, Australia) and miltefosine. For the COX activity assay, standard procedures provided by the manufacturer were followed. For COX inhibition, mitochondrial fractions were solubilized with 1 mM n-dodecyl- β -D-maltoside and total protein content was measured using the Better Bradford Assay Kit (Pierce, USA). The protein concentration of each mitochondrial preparation was adjusted to 4 $\mu\text{g}/\text{ml}$ using 1 \times enzyme dilution buffer supplied with the kit and a volume of 20 μl , equivalent to 80 ng of protein, was added to each reaction in a 96-well plate. KCN and miltefosine were diluted in 1 \times assay buffer and then mixed with reduced cytochrome c to give the series concentrations of KCN from 0 to 10 mM and miltefosine from 0 to 256 $\mu\text{g}/\text{ml}$ respectively, and a final reduced cytochrome c concentration of 20 μM . The total volume of each reaction was 220 μl and COX activity was monitored at 5 min intervals over a 4 h period at room temperature by measuring the absorbance at a wavelength of 550 nm (A_{550}) using a plate reader (Molecular Devices, USA, V max with SOFTmax PRO version 4.8) to determine the amount of reduced cytochrome c remaining in the reaction. The COX activity was calculated according to the definition of Sigma-Aldrich.

MOL #72322

Results

Miltefosine-Induced Mitochondrial Disruption and Apoptosis-Like Cell Death

We first determined the kinetics of cellular uptake of ^{14}C -labeled miltefosine by *S. cerevisiae*. Under the conditions specified, more than 60% of a saturating concentration of ^{14}C -miltefosine was taken up within 5 min, reaching a plateau within 10 to 20 min (Fig. 1A). To demonstrate that membrane-associated miltefosine was preferentially localized in mitochondria, we removed extracellular ^{14}C -miltefosine after 30 min in incubation by back-washing the cells with PBS containing 10 mg/ml BSA, disrupted the cell walls and prepared mitochondrial and membrane fractions by differential centrifugation as described in the Materials and Methods. Approximately 10% of the internalized drug was present in the mitochondrial fraction and 5% in the membrane fraction, confirming an enrichment in mitochondria (data not shown). To examine whether internalized miltefosine differentially targets metabolic pathways specific for fermentation or respiration, drug sensitivity of *S. cerevisiae* growing on different carbon sources was assessed. Yeast cells were reproducibly four times more sensitive to miltefosine in YPGly medium where the carbon source was non-fermentable glycerol, compared with cells growing in YPD where the carbon source was fermentable glucose. In YPGly cells were inhibited by a minimum 1 $\mu\text{g/ml}$ miltefosine, while in YPD cells were suppressed by a minimum 4 $\mu\text{g/ml}$ of the drug (Fig. 1B).

The effect of miltefosine on the function of mitochondria is shown in Figure 2. Healthy mitochondrial nucleoids in untreated cells were visualized microscopically by DAPI staining, as a bright punctate network of small spots. A tubular structure connecting the nucleoids was observed with DiOC₆, indicative of functional mitochondria with strong membrane potential. As

MOL #72322

expected, propidium iodide (PI), a non-membrane-permeable fluorescent dye, was not taken up by the untreated cells, indicative of cell viability.

After treatment with miltefosine for 1 h, three different cell populations were distinguishable by their staining patterns (Table 3). In the majority of the cells (approximately 68%), a diffuse DAPI and DiOC₆ staining pattern was observed, indicative of mitochondrial damage and disruption of mitochondrial membrane potential. However, this cell population was PI-negative, indicating that the cell membranes were physically intact. Only in a small population of the cells (approximately 13%), were the punctate structures of the mitochondria, as visualized with DAPI and DiOC₆, still visible although with reduced numbers of nucleoids, indicative of miltefosine-affected, but functional, mitochondria. Approximately 19% of the miltefosine-treated cells were PI positive, indicative of disrupted plasma membrane integrity and presumptively cell death. These cells were stained non-specifically with DAPI and DiOC₆ (Fig. 2).

To confirm that miltefosine induces apoptosis-like cell death in yeast, two intrinsic markers of apoptosis, caspase activation and nuclear DNA fragmentation, were sought in miltefosine-treated and untreated cells using flow cytometry and fluorescence microscopy (Fig. 3). Microscopic examination of spheroplasts subjected to TUNEL, revealed a subpopulation of cells with increased fluorescence following miltefosine treatment, indicative of TUNEL-specific DNA fragmentation. Activation of caspase was observed in miltefosine-treated whole cells. These results were confirmed by flow cytometry (Fig. 3).

Identifying *COX9* as a Potential Target of Miltefosine

To identify molecular targets of miltefosine, a genomic library housed within a high copy number shuttle vector, pCXJ15 (Chen, 1996), was constructed from a yeast strain, 6A-MI50-401.

MOL #72322

The library was then used to transform a wild type (WT) miltefosine sensitive strain, M2915-6A, to screen for clones conferring miltefosine resistance. Transformants were identified by their ability to grow in the presence of 20 $\mu\text{g/ml}$ miltefosine, a concentration of the drug 10 times greater than the MIC (Widmer et al., 2006a). Individual plasmids were isolated from miltefosine-resistant transformants and the DNA sequences of the inserts were determined. One of the plasmids contained a 1.8 kb DNA insert and a BLAST search against the *Saccharomyces cerevisiae* Genome Database revealed that it contained the gene *COX9* (Locus Tag: YDL067C, SGDID: S000002225) encoding the critical VIIa subunit (Cox9p) of the COX complex in the mitochondrial electron transport chain. This plasmid was later designated pCXJ15-COX9. DNA sequence analysis also confirmed that there was no mutation inadvertently introduced into the *COX9* fragment during the construction of the library, and that expression of *COX9* from the plasmid was regulated by its own native promoter and terminator.

To confirm that only the over-expression of *COX9* subunit in the COX complex confers resistance to miltefosine, two closely related genes, *COX7* and *COX8*, coding for adjacent subunits within the COX complex, were PCR amplified and cloned into pCXJ15, creating pCXJ15-COX7 and pCXJ15-COX8 respectively. Strain M2915-6A was transformed with pCXJ15-COX7, pCXJ15-COX8 and pCXJ15-COX9 individually. Over-expression of *COX7*, *COX8* and *COX9* in the Ura^+ transformants was confirmed by quantitative real time PCR (qRT-PCR). Results showed that the transcription levels of *COX7*, *COX8* and *COX9* were 9, 3.7 and 6.7-fold higher in the transformants carrying pCXJ15-COX7, pCXJ15-COX8 and pCXJ15-COX9 respectively, compared with the native levels in the control pCXJ15 transformants. 6A-[pCXJ15], 6A-[pCXJ15-COX7], 6A-[pCXJ15-COX8] and 6A-[pCXJ15-COX9] were examined on YNB plates, with or without 20 $\mu\text{g/ml}$ miltefosine, using a serial dilution drop test (Zuo et al.,

MOL #72322

2007). The miltefosine-resistant phenotype of yeast transformants containing pCXJ15-COX9 was confirmed and is shown in Figure 4. No miltefosine resistance was observed with transformants containing pCXJ15-COX7 or pCXJ15-COX8.

COX9 Gene Dosage and Cellular Respiration

To investigate the role of Cox9p in cellular respiration, a Δcox9 deletion mutant was generated from strain M2915-6A. Successful gene disruption was confirmed by PCR (Supplemental Figure 1). The resulting mutant, 6A/ Δcox9 , was tested for growth phenotype and respiratory competence on rich medium containing non-fermentable glycerol as the carbon source. The Δcox9 mutant failed to grow on YPGly despite prolonged incubation, indicative of a failure of respiration (Fig. 5). To determine whether the respiratory deficiency could be restored, the *COX9* gene was subcloned from the high copy number plasmid, pCXJ15-COX9, into a low copy number shuttle vector, pRS416 (Sikorski and Hieter, 1989) and both pRS416-COX9 and pCXJ15-COX9 were introduced into 6A/ Δcox9 . Ura⁺ transformants of Δcox9 -[pRS416-COX9] and Δcox9 -[pCXJ15-COX9] were then subcultured on YPGly for assessment of growth phenotype and respiratory competence. The low copy number plasmid, pRS416-COX9, complemented the respiratory deficiency of 6A/ Δcox9 , with the transformants exhibiting a similar growth rate to the parent strain, M2915-6A, and forming normal colonies on YPGly. Interestingly, the growth rate of Δcox9 -[pCXJ15-COX9] on YPGly was slower than Δcox9 -[pRS416-COX9] (Fig. 5).

To confirm that over-expression of *COX9* compromises growth and to investigate a possible gene dosage effect, the WT strain M2915-6A was transformed with pRS416-COX9 and pCXJ15-COX9, and Ura⁺ transformants of 6A-[pRS416-COX9] and 6A-[pCXJ15-COX9] were

MOL #72322

both assessed for growth on YPGly. While untransformed M2915-6A, containing only one copy of the native *COX9*, showed normal growth, colonies of the transformant 6A-[pRS416-COX9], containing both native *COX9* and a low copy number of pRS416-COX9, were slightly smaller than those of M2915-6A. 6A-[pCXJ15-COX9] containing multiple copies of *COX9* exhibited a qualitatively similar growth defect to that of Δcox9 -[pCXJ15-COX9].

Cox9p-Dependent Inhibition of COX by Miltefosine

To examine whether miltefosine treatment affects COX activity, mitochondria were isolated from the WT strain M2915-6A and subjected to a mild detergent treatment to release the COX complex from membrane lipid bilayers (Musatov et al., 2000). COX activity in the mitochondrial suspension was determined spectrophotometrically, using a Cytochrome c Oxidase Assay Kit (Sigma-Aldrich, Australia), to be approximately 0.25 units per milligram protein (Sigma-Aldrich definition). The mitochondrial suspension was then incubated with miltefosine at concentrations ranging from 0 to 256 $\mu\text{g/ml}$, or with the COX inhibitor, potassium cyanide (KCN) at concentrations ranging from 0 to 10 mM. The COX activity time courses clearly demonstrate that the enzyme in the WT strain was inhibited by both KCN and miltefosine in a dose-dependent manner (Fig. 6A-1 and Fig. 6B-1, respectively). While a high concentration of KCN (10 mM) caused a complete inhibition of the COX activity, a high dose of miltefosine (256 $\mu\text{g/ml}$) suppressed the enzyme by approximately 60%, reaching a level similar to the COX activity in the Δcox9 mutant (Fig. 6B-2).

To determine whether inhibition of COX by miltefosine is dependent on the presence of Cox9p, mitochondria prepared from 6A/ Δcox9 were examined for COX activity in the presence of the drug. When *COX9* was deleted from the genome, the activity of the COX was reduced to

MOL #72322

below 40% (Fig. 6B-2). Without Cox9p, the residual COX activity was inadequate to sustain aerobic cellular respiration, since 6A/ Δ cox9 was unable to grow on YPGly at 30 °C (Fig. 5). Importantly, in the absence of Cox9p the residual COX activity was not inhibited by miltefosine (Fig. 6B-2) but was suppressed by KCN (Fig. 6A-2).

To investigate the effect of *COX9* expression level on miltefosine-COX interaction, mitochondria from Δ cox9-[pRS416-COX9] were extracted and assayed for COX activity in the presence of miltefosine. Under conditions mimicking the endogenous expression level of Cox9p using the low copy number plasmid, the miltefosine-COX dose response was restored to WT level (Fig. 6B-4), consistent with the restoration of the growth phenotype observed on YPGly (Fig. 5) and indicative of a fully functional COX. The miltefosine-COX dose response observed in mitochondria derived from 6A-[pRS416-COX9], which carried low copies of *COX9* on the plasmid, did not differ significantly from that of the WT strain (Fig. 6B-3).

The COX activity of the mitochondria extracted from Δ cox9-[pCXJ15-COX9], where Cox9p was over-expressed due to multiple plasmid copies, was restored to approximately 70% of WT (Fig. 6B-6). However, mitochondria derived from 6A-[pCXJ15-COX9], which also contained over-expressed Cox9p, displayed similar COX activity to the WT mitochondria (Fig. 6B-5). Dose response of the enzyme to miltefosine from both transformants was evident.

MOL #72322

Discussion

Miltefosine is a potential lead compound for new antifungal drug development (Obando et al., 2007). It has clinically useful activity against another lower eukaryote, *Leishmania*, but undesirable toxicities (Sindermann and Engel, 2006). Understanding its mode of action is essential to the design of analogues with increased antifungal potency and reduced toxicity. Our data indicate that miltefosine induces apoptosis-like cell death in the model yeast, *S. cerevisiae*, as a result of a specific interaction with the Cox9p subunit of mitochondrial COX.

Miltefosine Penetrates Mitochondria and Disrupts Mitochondrial Function

Internalization of miltefosine by fungi has not previously been studied directly, although it has been shown in *S. cerevisiae* that fluorescently labeled analogues of PC are transported across the plasma membrane to the cytosolic leaflet by a protein-mediated, energy-dependent mechanism and that these analogues are distributed subsequently to the nuclear envelope/ER and mitochondria (Grant et al., 2001). The protein Lem3p was later identified as a specific membrane transporter for PC, PE and, presumptively, miltefosine, since deletion of *LEM3* conferred resistance to miltefosine (Hanson et al., 2003). *LEM3* is a member of an evolutionarily conserved gene family and has two homologues in *S. cerevisiae*.

In the present study, uptake of ^{14}C -miltefosine by yeast cells was very rapid and reached plateau within 10 to 20 min. This is consistent with internalization of miltefosine via a saturable, active transport channel, presumably involving Lem3p. Since mitochondria are widely distributed double-membrane networks within cells and form a large part of the cellular membrane system, it is probable that, following internalization, miltefosine distributes along the

MOL #72322

lipid bilayers of the mitochondria and interacts with potential drug targets, both on the membranes and in the matrix. Our data indeed showed that more than 10% of internalized ^{14}C -miltefosine localized to subcellular mitochondrial fraction of the cell lysates.

An effect of miltefosine on mitochondrial function was clearly demonstrated since yeast cells growing by respiration, relying heavily on mitochondrial function, were four times more sensitive to miltefosine than cells growing by fermentation (Fig 1B).

A selective effect of miltefosine on mitochondria was demonstrated by staining cells with DAPI and DiOC₆, which revealed that miltefosine penetrated into the mitochondrial inner membrane causing disruption of the membrane potential and dispersal of mitochondrial nucleoids within the matrix (Fig. 2).

Miltefosine Causes Apoptosis-Like Cell Death in Yeast

There is little doubt that miltefosine causes apoptosis in both cancer cells and leishmanial parasites (Barratt et al., 2009). However, the biochemical basis of apoptosis in these cells, in particular whether it occurs as a direct consequence of inhibition of PC synthesis, remains controversial (van der Sanden et al., 2004).

Apoptosis has been reported in a range of yeast including *S. cerevisiae*, *Schizosaccharomyces pombe* and *Candida albicans* (Ramsdale, 2008). *S. cerevisiae* has been used as the model system since the characterization of the *CDC48* mutation that led to the discovery of apoptosis in yeasts (Madeo et al., 2004). Genes involved in programmed cell death in *S. cerevisiae* have also been identified as apoptotic regulators in mammalian cells, indicating that the basic apoptotic machinery is indeed present and functional.

MOL #72322

In the present study, a miltefosine concentration at 2 $\mu\text{g/ml}$ clearly caused apoptosis-like cell death, as demonstrated by disruption of mitochondrial function and miltefosine-induced nuclear damage (Fig. 2). TUNEL-specific fragmentation of DNA and activation of cellular caspases were obvious in miltefosine-treated cell cultures (Fig 3). These observations are typical signs of apoptosis in yeast (Thevissen et al., 2008). Furthermore, miltefosine directly inhibited COX located on the mitochondrial inner membrane (Fig. 6). Our results suggest that, as a result of direct interaction between the drug and COX, miltefosine disrupts mitochondrial homeostasis and triggers apoptotic signaling.

Cox9p Is the Inhibition Site of COX by Miltefosine

The COX enzyme complex catalyses the final step of respiration, transferring electrons from cytochrome c to molecular oxygen. By coupling electron transfer to proton translocation from the mitochondrial matrix to the intermembrane space, COX maintains the electrochemical potential required by the oxidative phosphorylation system for the synthesis of ATP. As most human invasive fungal pathogens grow only by cellular respiration, fungus-specific components of the COX complex would be potentially novel antifungal drug targets. Our data demonstrate that the inhibition of COX activity by miltefosine is dose-dependent and relies on the presence of Cox9p (Fig. 6). As possible Cox9p homologues in other eukaryotes have substantially diverged from those in fungi, Cox9p is potentially a fungus-specific subunit of the COX complex targetable by the drugs.

As COX is a polymeric enzyme, with subunits encoded by either the nucleus or the mitochondria, its assembly is complex, highly regulated, and requires coordination between both organelles (Fontanesi et al., 2006). Crystallization of bovine COX has provided a detailed insight

MOL #72322

into its three-dimensional organization (Tsukihara et al., 1996). In *S. cerevisiae*, 11 subunits of the enzyme complex have been identified. Three large subunits, Cox1p, Cox2p and Cox3p which form the catalytic core, are encoded by the mitochondrial genome and synthesized within the matrix. It has been reported that the catalytic core is embedded within the inner membrane. The heme and copper cofactors, which are involved in the electron transport activity of the COX complex, are coordinated by Cox1p and Cox2p. Other small subunits, including Cox7p, Cox8p and Cox9p, are nuclear-encoded, synthesized in the cytoplasm and imported into the mitochondria. These small subunits are associated with the hydrophobic core and are essential for the assembly and stability of the holoenzyme. The small subunits are also involved in the modulation of catalytic activity and protection of the core from damaging reactive oxygen species.

In this study, *COX9* was isolated from a genetic screen for possible molecular targets of miltefosine. *COX9* has previously been cloned and is present as a single copy in the haploid genome of *S. cerevisiae* (Wright et al., 1986). Our results demonstrate that Cox9p is essential for maintaining a fully functional COX assembly and that the level of Cox9p expression impacts on yeast cellular respiration (Fig. 5). In the Δ *cox9* mutant, the growth arrest correlated with a greater than 60% loss of COX activity, indicating that this level of COX inhibition was sufficient to prevent oxidative phosphorylation. This level of inhibition was also detected in WT COX treated with high concentrations of miltefosine. In the absence of Cox9p, the remaining COX activity was not further inhibited by miltefosine, but was sensitive to KCN, implicating Cox9p as the site within COX responsible for the miltefosine dose-dependent inhibition (Fig. 6).

Restoration of Cox9p expression in the Δ *cox9* mutant by an exogenous *COX9* in low copy number completely restored COX functionality and cellular respiration. The miltefosine-COX

MOL #72322

dose response of the transformants was also similar to that of WT COX. Over-expression of Cox9p in 6A-[pCXJ15-COX9] and Δ cox9-[pCXJ15-COX9] resulted in defective growth on non-fermentable carbon source, suggesting that the *COX9* copy number is crucial for optimal cellular respiration and hence growth, and that over-expression of the gene is detrimental. COX activity in the *COX9* over-expression strain 6A-[pCXJ15-COX9] was similar to that of the WT strain, but in Δ cox9-[pCXJ15-COX9] it was 70% of WT. Although this result might indicate a biased preference by the COX for chromosomally expressed Cox9p, when Cox9p was over-expressed, there was a clear miltefosine-COX dose response. Taken together, these results indicate that regulation of the cellular level of Cox9p is critical for optimal COX function, and that changes in Cox9p levels likely render the COX complex unstable.

It has been proposed that mature Cox9p is a 6.3 kDa amphiphilic peptide of 54 amino acids, with an internal hydrophobic domain and hydrophilic *N*- and *C*-termini. This structural motif is similar to that of Cox7p and Cox8p. Cox9p, together with Cox7p and Cox8p, form a transmembrane intermediate subassembly that spans the lipid bilayer of the inner membrane (Power et al., 1986) and is therefore accessible to miltefosine. Our results showed that over-expression of only Cox9p, but not Cox7p and Cox8p, confers miltefosine resistance in yeast cells. It seems likely that miltefosine-Cox9p binding reduces the amount of Cox9p available for assembly of functional enzyme complexes; hence COX becomes structurally unstable and vulnerable to proteolysis. Plasmid-derived Cox9p can compensate for the loss of native Cox9p bound to miltefosine, as transformants containing pCXJ15-COX9 were resistant to miltefosine, while cells with pCXJ15-COX7 or pCXJ15-COX8 were still sensitive to the drug (Fig. 4).

MOL #72322

In summary, we conclude that Cox9p is a target of the antifungal drug miltefosine. We propose that interaction between Cox9p and miltefosine disrupts the electron transport chain by causing partial disassembly of COX, ultimately leading to an apoptosis-like cell death.

MOL #72322

Acknowledgement

We thank J. Munro, M. Karam, N. Pantarat, C. Biswas, C. F. Wilson, Y. Koda, F. Widmer and H. Yu for technical assistance and advice. We also thank S. Lev for proofreading of the manuscript.

MOL #72322

Authorship Contributions

Participated in research design: Zuo, Djordjevic, Sorrell and Jolliffe

Conducted experiments: Zuo, Bijosono Oei, Desmarini and Schibeci

Performed data analysis: Zuo, Djordjevic, Schibeci and Sorrell

Wrote or contributed to the writing of the manuscript: Zuo, Djordjevic, Sorrell and Jolliffe

MOL #72322

References

- Barcellona ML, Cardiel G and Gratton E (1990) Time-resolved fluorescence of DAPI in solution and bound to polydeoxynucleotides. *Biochem Biophys Res Commun* **170**:270-280.
- Barratt G, Saint-Pierre-Chazalet M and Loiseau PM (2009) Cellular transport and lipid interactions of miltefosine. *Curr Drug Metab* **10**:247-255.
- Burke D, Dawson D and Stearns T (2000) *Methods in yeast genetics : a Cold Spring Harbor Laboratory course manual*. Cold Spring Harbor Laboratory Press, Cold Spring Harbor, N.Y.
- Chen SC and Sorrell TC (2007) Antifungal agents. *Med J Aust* **187**:404-409.
- Chen XJ (1996) Low- and high-copy-number shuttle vectors for replication in the budding yeast *Kluyveromyces lactis*. *Gene* **172**:131-136.
- Chen XJ, Guan MX and Clark-Walker GD (1993) *MGM101*, a nuclear gene involved in maintenance of the mitochondrial genome in *Saccharomyces cerevisiae*. *Nucleic Acids Res* **21**:3473-3477.
- Clark-Walker GD, Hansbro PM, Gibson F and Chen XJ (2000) Mutant residues suppressing ρ^0 -lethality in *Kluyveromyces lactis* occur at contact sites between subunits of F_1 -ATPase. *Biochim Biophys Acta* **1478**:125-137.
- Croft SL, Seifert K and Duchene M (2003) Antiprotozoal activities of phospholipid analogues. *Mol Biochem Parasitol* **126**:165-172.
- de Castro SL, Santa-Rita RM, Urbina JA and Croft SL (2004) Antiprotozoal lysophospholipid analogues: a comparison of their activity against trypanosomatid parasites and tumor cells. *Mini Rev Med Chem* **4**:141-151.

MOL #72322

Fontanesi F, Soto IC, Horn D and Barrientos A (2006) Assembly of mitochondrial cytochrome c-oxidase, a complicated and highly regulated cellular process. *Am J Physiol Cell Physiol* **291**:C1129-1147.

Grant AM, Hanson PK, Malone L and Nichols JW (2001) NBD-labeled phosphatidylcholine and phosphatidylethanolamine are internalized by transbilayer transport across the yeast plasma membrane. *Traffic* **2**:37-50.

Hanson PK, Malone L, Birchmore JL and Nichols JW (2003) Lem3p is essential for the uptake and potency of alkylphosphocholine drugs, edelfosine and miltefosine. *J Biol Chem* **278**:36041-36050.

Jauert PA, Jensen LE and Kirkpatrick DT (2005) A novel yeast genomic DNA library on a geneticin-resistance vector. *Yeast* **22**:653-657.

Kesson AM, Bellemore MC, O'Mara TJ, Ellis DH and Sorrell TC (2009) *Scedosporium prolificans* osteomyelitis in an immunocompetent child treated with a novel agent, hexadecylphosphocholine (miltefosine), in combination with terbinafine and voriconazole: a case report. *Clin Infect Dis* **48**:1257-1261.

Lux H, Heise N, Klenner T, Hart D and Opperdoes FR (2000) Ether-lipid (alkyl-phospholipid) metabolism and the mechanism of action of ether-lipid analogues in *Leishmania*. *Mol Biochem Parasitol* **111**:1-14.

Madeo F, Herker E, Wissing S, Jungwirth H, Eisenberg T and Frohlich KU (2004) Apoptosis in yeast. *Curr Opin Microbiol* **7**:655-660.

Musatov A, Ortega-Lopez J and Robinson NC (2000) Detergent-solubilized bovine cytochrome c oxidase: dimerization depends on the amphiphilic environment. *Biochemistry* **39**:12996-13004.

MOL #72322

Obando D, Widmer F, Wright LC, Sorrell TC and Jolliffe KA (2007) Synthesis, antifungal and antimicrobial activity of alkylphospholipids. *Bioorg Med Chem* **15**:5158-5165.

Perez-Victoria FJ, Gamarro F, Ouellette M and Castanys S (2003) Functional cloning of the miltefosine transporter. A novel P-type phospholipid translocase from *Leishmania* involved in drug resistance. *J Biol Chem* **278**:49965-49971.

Power SD, Lochrie MA and Poyton RO (1986) The nuclear-coded subunits of yeast cytochrome c oxidase. The amino acid sequences of subunits VII and VIIa, structural similarities between the three smallest polypeptides of the holoenzyme, and implications for biogenesis. *J Biol Chem* **261**:9206-9209.

Pringle JR, Preston RA, Adams AE, Stearns T, Drubin DG, Haarer BK and Jones EW (1989) Fluorescence microscopy methods for yeast. *Methods Cell Biol* **31**:357-435.

Ramsdale M (2008) Programmed cell death in pathogenic fungi. *Biochim Biophys Acta* **1783**:1369-1380.

Ruiter GA, Zerp SF, Bartelink H, van Blitterswijk WJ and Verheij M (1999) Alkyllysophospholipids activate the SAPK/JNK pathway and enhance radiation-induced apoptosis. *Cancer Res* **59**:2457-2463.

Sambrook J, Russell DW and Cold Spring Harbor Laboratory. (2001) *Molecular cloning : a laboratory manual*. Cold Spring Harbor Laboratory, Cold Spring Harbor, N.Y.

Sikorski RS and Hieter P (1989) A system of shuttle vectors and yeast host strains designed for efficient manipulation of DNA in *Saccharomyces cerevisiae*. *Genetics* **122**:19-27.

Sindermann H and Engel J (2006) Development of miltefosine as an oral treatment for leishmaniasis. *Trans R Soc Trop Med Hyg* **100 Suppl 1**:S17-20.

MOL #72322

- Thevissen K, Madeo F, Ludovico P, Cammue B and Winderickx J (2008) Joined in death: highlights of the Sixth International Meeting on Yeast Apoptosis in Leuven, Belgium, 30 April-4 May 2008. *Yeast* **25**:927-934.
- Tong Z, Widmer F, Sorrell TC, Guse Z, Jolliffe KA, Halliday C, Lee OC, Kong F, Wright LC and Chen SC (2007) *In vitro* activities of miltefosine and two novel antifungal biscationic salts against a panel of 77 dermatophytes. *Antimicrob Agents Chemother* **51**:2219-2222.
- Tsukihara T, Aoyama H, Yamashita E, Tomizaki T, Yamaguchi H, Shinzawa-Itoh K, Nakashima R, Yaono R and Yoshikawa S (1996) The whole structure of the 13-subunit oxidized cytochrome c oxidase at 2.8 Å. *Science* **272**:1136-1144.
- Unger C and Eibl H (1991) Hexadecylphosphocholine: preclinical and the first clinical results of a new antitumor drug. *Lipids* **26**:1412-1417.
- Urbina JA (2006) Mechanisms of action of lysophospholipid analogues against trypanosomatid parasites. *Trans R Soc Trop Med Hyg* **100 Suppl 1**:S9-S16.
- van Blitterswijk WJ and Verheij M (2008) Anticancer alkylphospholipids: mechanisms of action, cellular sensitivity and resistance, and clinical prospects. *Curr Pharm Des* **14**:2061-2074.
- van der Sanden MH, Houweling M, Duijsings D, Vaandrager AB and van Golde LM (2004) Inhibition of phosphatidylcholine synthesis is not the primary pathway in hexadecylphosphocholine-induced apoptosis. *Biochim Biophys Acta* **1636**:99-107.
- Verma NK, Singh G and Dey CS (2007) Miltefosine induces apoptosis in arsenite-resistant *Leishmania donovani* promastigotes through mitochondrial dysfunction. *Exp Parasitol* **116**:1-13.

MOL #72322

- Wach A, Brachat A, Pohlmann R and Philippsen P (1994) New heterologous modules for classical or PCR-based gene disruptions in *Saccharomyces cerevisiae*. *Yeast* **10**:1793-1808.
- Widmer F, Hartmann M, Frey B and Kolliker R (2006a) A novel strategy to extract specific phylogenetic sequence information from community T-RFLP. *J Microbiol Methods* **66**:512-520.
- Widmer F, Wright LC, Obando D, Handke R, Ganendren R, Ellis DH and Sorrell TC (2006b) Hexadecylphosphocholine (miltefosine) has broad-spectrum fungicidal activity and is efficacious in a mouse model of cryptococcosis. *Antimicrob Agents Chemother* **50**:414-421.
- Wieder T, Reutter W, Orfanos CE and Geilen CC (1999) Mechanisms of action of phospholipid analogs as anticancer compounds. *Prog Lipid Res* **38**:249-259.
- Wright RM, Dircks LK and Poyton RO (1986) Characterization of *COX9*, the nuclear gene encoding the yeast mitochondrial protein cytochrome c oxidase subunit VIIa. Subunit VIIa lacks a leader peptide and is an essential component of the holoenzyme. *J Biol Chem* **261**:17183-17191.
- Zuo X, Xue D, Li N and Clark-Walker GD (2007) A functional core of the mitochondrial genome maintenance protein Mgm101p in *Saccharomyces cerevisiae* determined with a temperature-conditional allele. *FEMS Yeast Res* **7**:131-140.

MOL #72322

Footnotes

This work was supported by the National Health and Medical Research Council, Australia [Project Grant 570891]. T.C.S. was supported by a Fellowship from the Sydney Medical School Foundation.

MOL #72322

Legends for Figures

Fig. 1. Miltefosine incorporation into yeast and their drug sensitivity. *A:* Yeast cells cultured to late log phase in YNB broth were incubated with 1 $\mu\text{g/ml}$ ^{14}C -labeled miltefosine at 30°C for the times indicated. At each time point the cell-associated ^{14}C -miltefosine was measured by scintillation counting. Error bars represent the standard deviation ($n = 3$). Note that over 60% of the drug was incorporated into the cells within 5 min. *B:* In a 96-well plate, 100 μl /well of YPD or YPGly broth containing miltefosine at the concentrations indicated was inoculated with 5×10^3 yeast cells in each well. The plate was then incubated at 30°C with vigorous shaking until the growth of the cells had reached the final stage (4 days). Note that turbidity within a well is indicative of cell growth that is not inhibited by the drug. White circles indicate the wells containing the minimum concentrations of miltefosine required to inhibit cell growth.

Fig. 2. Disruption of mitochondrial function by miltefosine. Yeast cells were incubated with 2 $\mu\text{g/ml}$ miltefosine in YPD broth for 1 h, and stained with DAPI (to visualize mitochondrial and nuclear DNA), DiOC₆ (to visualize mitochondrial membrane potential) and PI (to detect cell viability via cell membrane permeability). Controls (marked as Untreated) contained no miltefosine. Fluorescence microscope images show that miltefosine treatment disrupted mitochondrial membrane potential (lower panel of DiOC₆ staining), diffused mitochondrial nucleoids (lower panel of DAPI staining) and increased membrane permeability (lower panel of PI staining).

MOL #72322

Fig. 3. Apoptosis caused by miltefosine. Cells were treated with 2 $\mu\text{g/ml}$ miltefosine or no drug at 30°C for 4 h, and examined for TUNEL or caspase activation by fluorescence microscopy and flow cytometry. For the TUNEL assay cells were fixed with paraformaldehyde and spheroplasted before labeling. Representative views of the microscopy are shown. Dot plots of fluorescence intensity verses side scatter (SSC) obtained with flow cytometry demonstrate that, in miltefosine-treated samples, 12% of the cells were caspase-activated and 40% of the cells were TUNEL-positive.

Fig. 4. Miltefosine resistance conferred by *COX9* over-expression. YNB plates containing 20 $\mu\text{g/ml}$ miltefosine or no drug with drops of serially diluted M2915-6A transformants of pCXJ15-COX7, pCXJ15-COX8 and pCXJ15-COX9 are shown. 6A-[pCXJ15] was used for comparison. Photos were taken with a PowerShot A720 IS digital camera (Canon, Japan) after incubation at 30°C for 3 days. Note that only 6A-[pCXJ15-COX9] showed miltefosine resistance.

Fig. 5. *COX9* gene dosage on cellular respiration. Growth of the Δcox9 mutant and its parental strain on YPD (left panels) and YPGly (right panels) are shown. The effect of gene dosage is present in strains transformed with either a low copy number plasmid pRS416-COX9 or a high copy number plasmid pCXJ15-COX9 (as indicated in the square brackets). Following 5-day incubation at 30°C, photos were taken using a digital camera. Note that a functional *COX9* on a low copy number plasmid restored respiration in the Δcox9 mutant. Respiration was reduced in transformants containing more than one copies of *COX9*.

MOL #72322

Fig. 6. Cox9p-dependent miltefosine-COX dose response. Mitochondrial fractions were extracted from the strains indicated, and dissolved in enzyme dilution buffer with 1 mM n-dodecyl- β -D-maltoside. COX activity in the mitochondria was measured using a Cytochrome c Oxidase Assay Kit. *A*: Time courses of COX inhibition by KCN at various concentrations are shown, taking samples with no COX as controls. Note that, in the absence of Cox9p, the remaining COX activity in 6A/ Δ cox9 was still sensitive to KCN. *B*: Time courses of COX activity at different concentration of miltefosine are shown. Controls without COX are labeled as Ctrl. Note that miltefosine inhibited COX in a dose-dependent manner only when Cox9p was present.

MOL #72322

Tables

Table 1. Yeast strains used in this work

Name	Description	Source
M2915-6A	<i>MATa, leu2, ade2, ura3</i>	Chen et al., 1993
6A-MI50-401	<i>MATa, leu2, ade2, ura3</i> , miltefosine resistant	This study
6A-[pCXJ15]	M2915-6A transformed with pCXJ15	This study
6A-[pCXJ15-COX7]	M2915-6A transformed with pCXJ15-COX7	This study
6A-[pCXJ15-COX8]	M2915-6A transformed with pCXJ15-COX8	This study
6A-[pCXJ15-COX9]	M2915-6A transformed with pCXJ15-COX9	This study
6A-[pRS416-COX9]	M2915-6A transformed with pRS416-COX9	This study
BY4741/ Δ cox9	<i>MATa, his3, leu2, met15, ura3, cox9Δ::KanMX4</i>	Open Biosystems, USA
6A/ Δ cox9	M2915-6A with <i>cox9Δ::KanMX4</i>	This study
Δ cox9-[pRS416-COX9]	6A/ Δ cox9 transformed with pRS416-COX9	This study
Δ cox9-[pCXJ15-COX9]	6A/ Δ cox9 transformed with pCXJ15-COX9	This study

MOL #72322

Table 2. PCR primers used in this work

Name	Used for	Nucleotide Sequence (5' – 3')
ScCOX7 FP1	Cloning of <i>COX7</i>	CCCGGGGAATTTCGGAGGAGTAATCTTTTCAGT
ScCOX7 RP1	Cloning of <i>COX7</i>	CCCGGGGAATTCCACAAGAATCAACAGCAACA
ScCOX8 FP1	Cloning of <i>COX8</i>	CCCGGGGAATTCAATGCAAGCATCAAGAGCAA
ScCOX8 RP1	Cloning of <i>COX8</i>	CCCGGGGAATTCACTCATTGCAACAAAGTAAACTGC
Sc <i>cox9</i> FP1	Disruption of <i>COX9</i>	GGATTGTAAGACACCTTTAT
Sc <i>cox9</i> RP1	Disruption of <i>COX9</i>	CTGTCTTATTCTCCACATACA
Sc <i>cox9</i> FP2	Confirmation of Δ <i>cox9</i>	ATACTCATGCTGGGCGATCT
Sc <i>cox9</i> RP2	Confirmation of Δ <i>cox9</i>	GATGGGAATATACCTGCGAA
ScACT1 QRP1	qRT-PCR for <i>ACT1</i>	ACGTGAGTAACACCATCACCGGAA
ScACT1 QFP1	qRT-PCR for <i>ACT1</i>	ACGTTCCAGCCTTCTACGTTTCCA
ScCOX7 QRP1	qRT-PCR for <i>COX7</i>	TAGAAGTGGTGTAACGACGGCTAC
ScCOX7 QFP1	qRT-PCR for <i>COX7</i>	CTATGGTGGAGACATCCAAGGTCA
ScCOX8 QRP1	qRT-PCR for <i>COX8</i>	GCAAATCCAATAGCGAAGAACCCG
ScCOX8 QFP1	qRT-PCR for <i>COX8</i>	GAGGTCAGTACACTTCAAAGACGGTG
ScCOX9 QRP1	qRT-PCR for <i>COX9</i>	GCTAGCTCTGCGTAGAACTTCTCT
ScCOX9 QFP1	qRT-PCR for <i>COX9</i>	AGAGTCATCATGGACATCGTCCTC

Italicized nucleotides in the primers are the sequences matching the yeast genome.

MOL #72322

Table 3. Microscopic assessment of mitochondrial disruption by miltefosine

	Untreated	Miltefosine-treated^a
PI ^[−] cells with healthy mitochondria ^b (%)	≥98.0	12.8±1.0
PI ^[−] cells with disrupted mitochondria ^c (%)	≤2.0	68.2±1.8
PI ^[+] cells ^d (%)	≤0.3	19.0±2.4

a. Average cell numbers with standard deviation (n = 3) are presented.

b. Functional mitochondria are shown in Figure 2 as networks of punctate bright spots (DAPI) connected by tubular structures (DiOC₆).

c. Disrupted mitochondria have a diffuse staining pattern in Figure 2 with both DAPI and DiOC₆ staining.

d. PI^[+] cells are presumed dead.

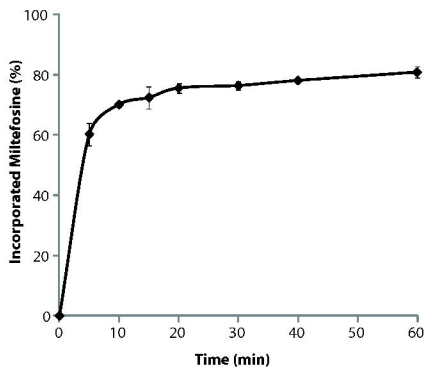
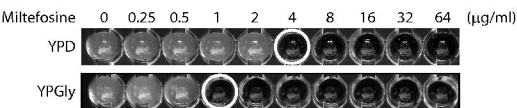
A**B**

Figure 1

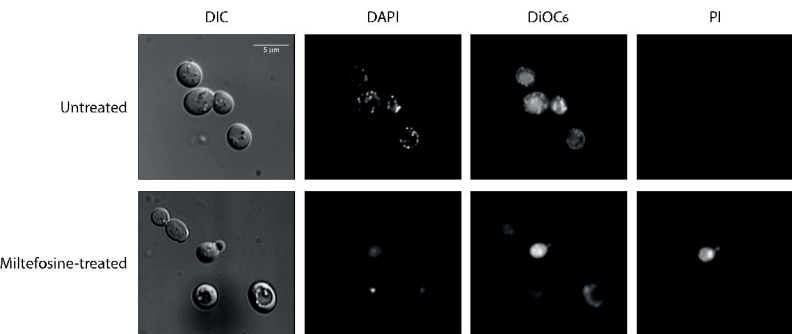


Figure 2

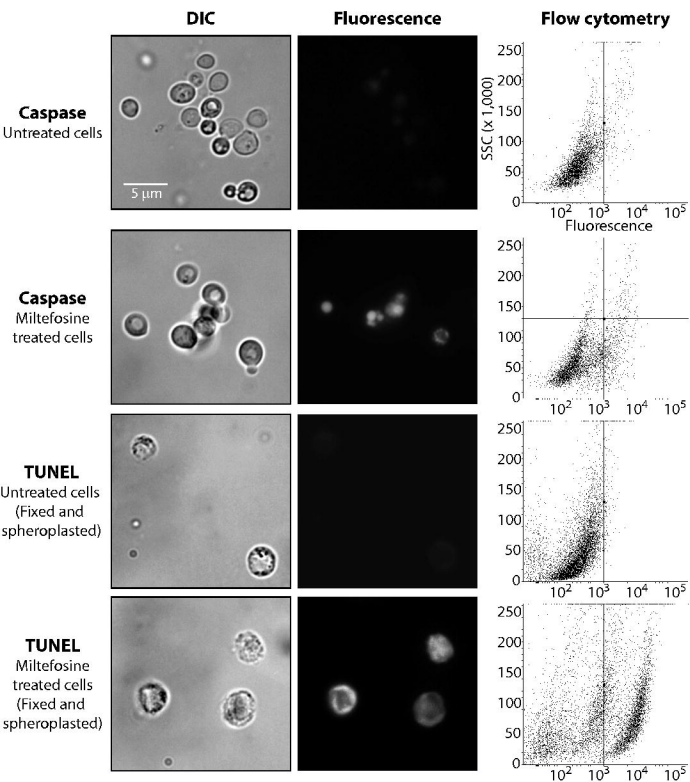


Figure 3

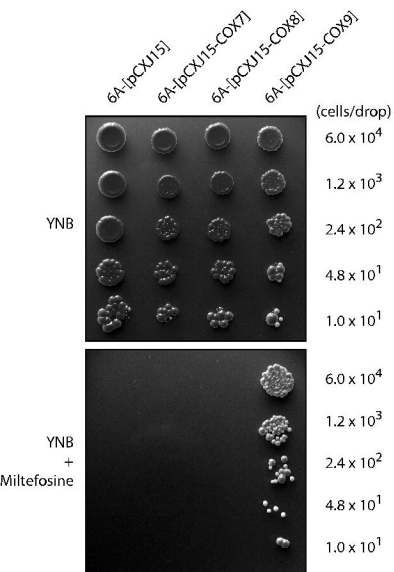


Figure 4

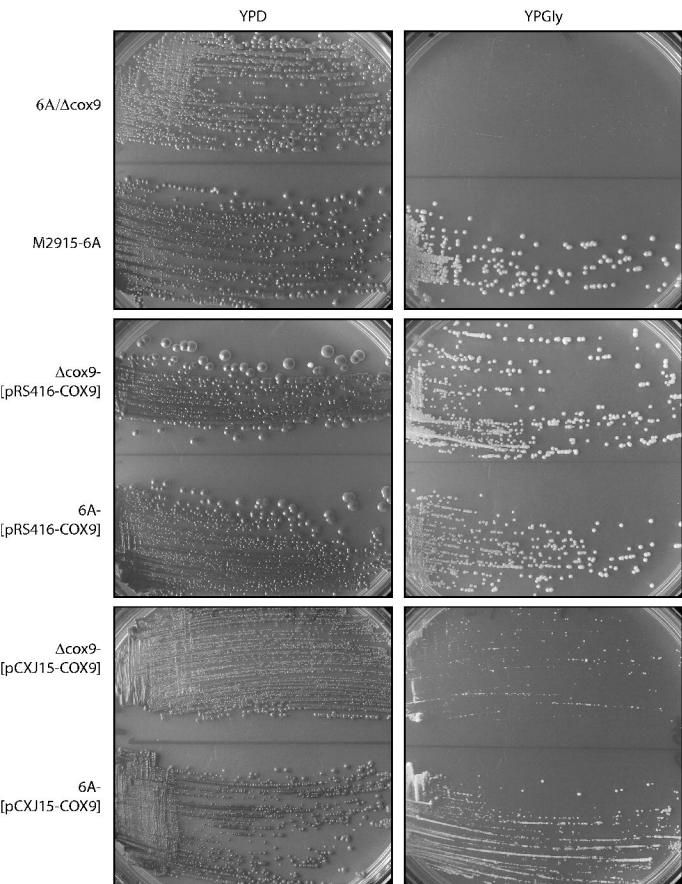
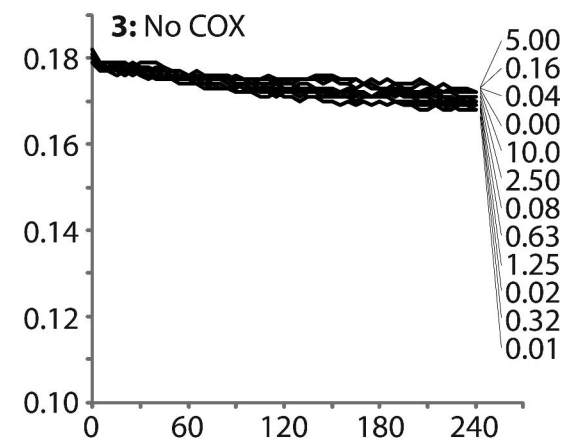
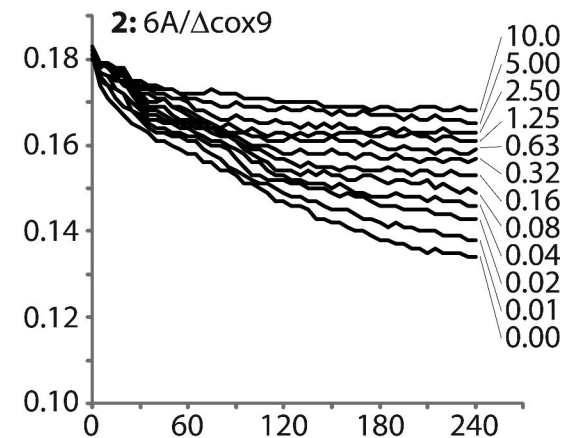
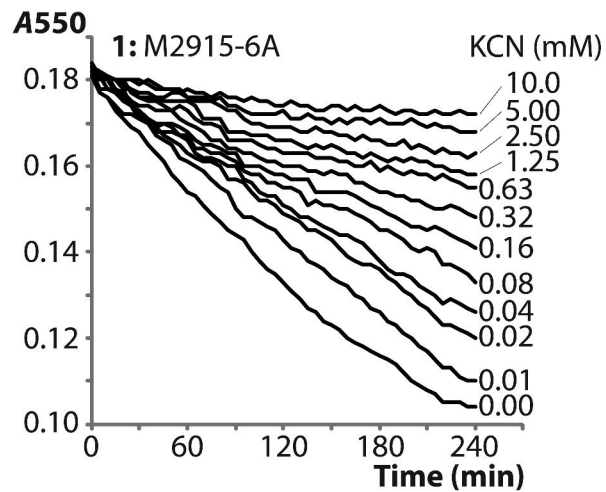
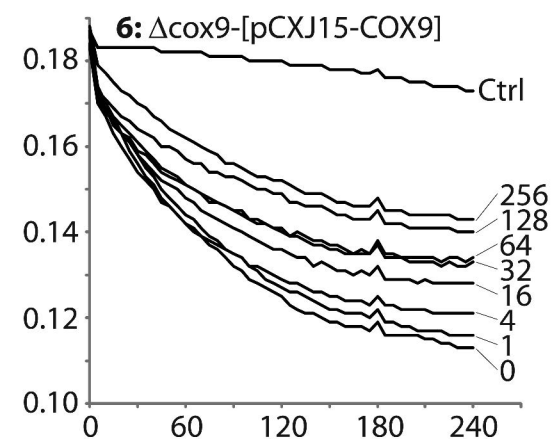
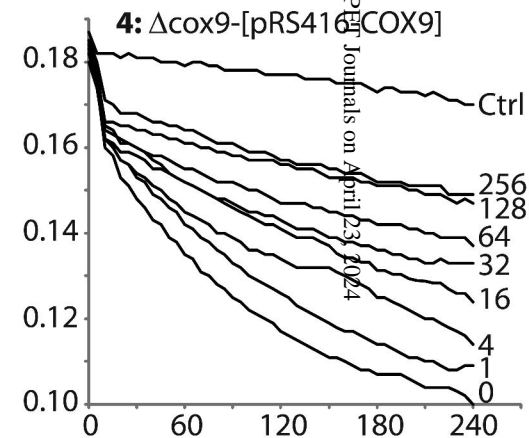
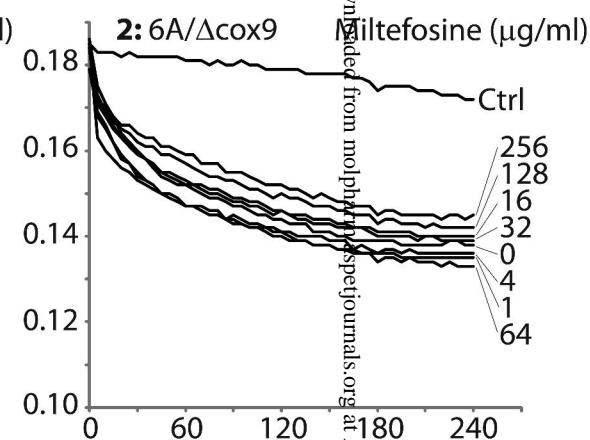
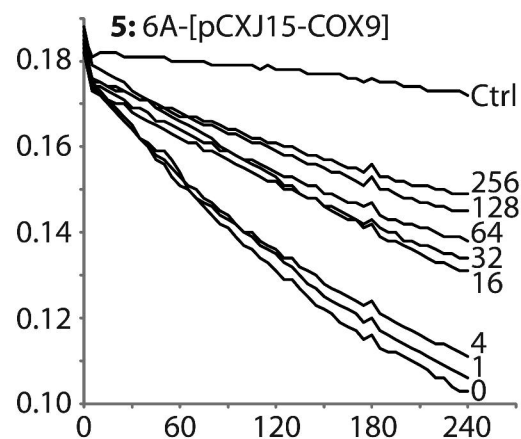
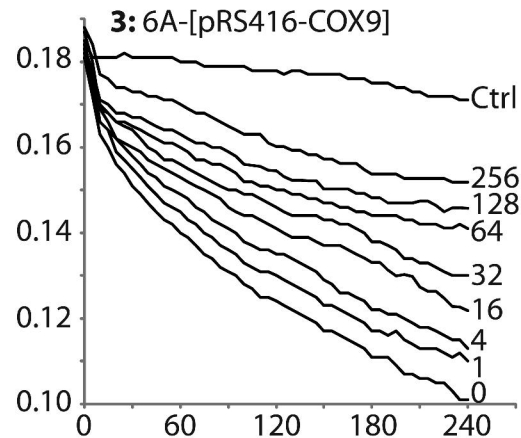
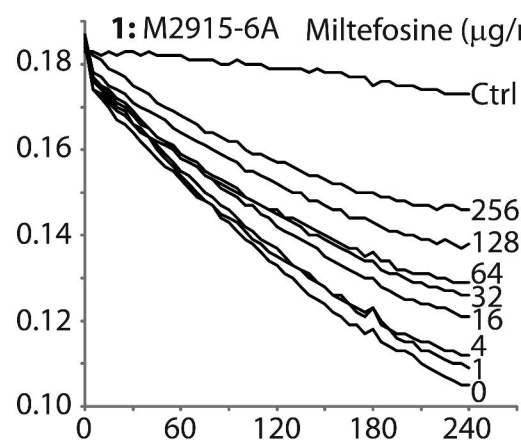
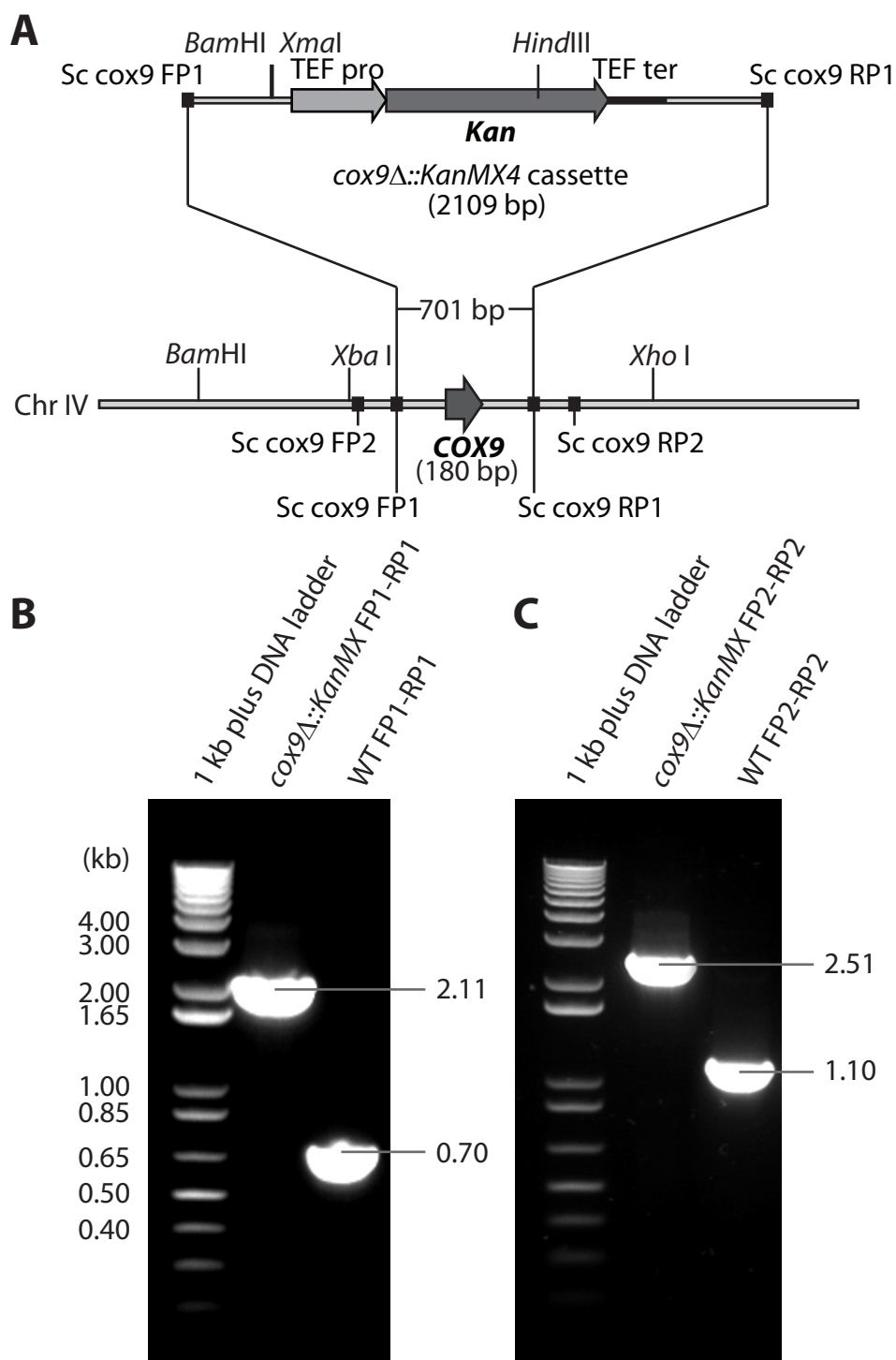


Figure 5

A: KCN-COX interaction**B: Miltefosine-COX interaction**

Downloaded from molpharm.aspetjournals.org at ASPET Journals on April 23, 2024



Supplemental Figure 1. Deletion of *COX9* in M2915-6A. **A:** Physical map of the *cox9Δ::KanMX4* cassette and the disruption locus of the *S. cerevisiae* chromosome IV. **B:** PCR amplification of the *cox9Δ::KanMX4* cassette from BY4741/ Δ *cox9* using Sc *cox9* FP1 and Sc *cox9* RP1 showed a product of 2109 bp (*cox9Δ::KanMX4* FP1-RP1), while amplification from M2915-6A yielded a product of 701 bp (WT FP1-RP1). **C:** After the disrupting cassette was integrated into the chromosome, PCR confirmation of the *cox9* deletion in 6A/ Δ *cox9* using Sc *cox9* FP2 and Sc *cox9* RP2 showed an amplicon of 2509 bp (*cox9Δ::KanMX4* FP2-RP2) instead of 1101 bp in the parental strain (WT FP2-RP2).